IMPEDANCE MEASUREMENTS OF THE LEAD/SODIUM SULPHATE SYSTEM: SYNTHESIS OF a.c. ANALOGUE CIRCUIT

M. BOJINOV* and B. MONAHOV

Central Laboratory of Electrochemical Power Sources, Bulgarian Academy of Sciences, Sofia 1040 (Bulgaria)

Introduction

Lead forms different electrode systems in aqueous solutions containing sulphate ions; the stability of these systems depends on the pH and the applied potential. Most of the systems have theoretical and practical importance through their participation in the various operational stages of the lead/acid battery.

The a.c. impedance method for investigating electrode kinetics is often used for the identification of complex electrochemical reactions that proceed via more than one elementary step and include both liquid and solid diffusion-limited processes. The impedance technique also allows a characterization to be made of the metal/solid-electrolyte and semiconductor/electrolyte interfaces [1 - 11]. Complex, non-stationary systems, such as the Pb/PbO electrode in sulphate ion-containing aqueous solutions with various pH, can be defined through combining impedance studies with voltammetric, photovoltammetric, and X-ray diffraction techniques.

a.c. Impedance investigations of the various electrode systems existing in the lead/acid cell have been performed by a number of authors [12 - 18]. In particular, studies have been conducted [12 - 15] of the influence of different alloying elements on the formation and reduction of PbO_2. An a.c. analogue circuit of the system $Pb/PbO_2/PbSO_4/H_2SO_4$ has been developed in which the capacity and resistance of the sulphate layer are connected in series with the Pb/PbO_2 interfacial impedance (including the double-layer capacitance in parallel with a charge-transfer/diffusion controlled faradaic reaction of PbO_2 formation/reduction). Analogue circuits have also been developed for the $Pb/PbSO_4/H_2SO_4$ system at open-circuit potential as well as under cathodic (lead sulphate reduction) or anodic (formation and properties of lead sulphate layer) d.c. polarization [16, 17]. An attempt at developing an a.c. circuit describing the electrochemical properties of the $Pb/PbO/PbSO_4/H_2SO_4$ electrode has been made [18] using constant phase-angle (CPA) impedance [10].

---

*Author to whom correspondence should be addressed.

It is well known that lead oxide can be considered to be either a solid electrolyte in which the oxygen vacancies are the major charge carriers [19, 20] or a semiconductor [21]. The basic purpose of the work reported here is to determine the solid electrolyte and semiconductor properties of the PbO layer.

The electrode system formed on the lead electrode during anodic polarization in sulphuric acid can be written as $Pb/PbO/PbSO_4/H_2SO_4$ solution. This system is considered to be non-stationary because of the complexity of the processes at the oxide-layer:sulphate-layer/sulphuric-acid interface. Therefore, it is necessary to eliminate the lead sulphate influence in order to clarify the role of the Pb/PbO interface in the overall oxidation reaction. Since high pH values result in oxide-film formation, Na_2SO_4 solution is used as the forming electrolyte. It is assumed that neither Na^+ nor SO_4^{2-} ions take part in the electrode reactions that are proceeding in nearly neutral solutions.

Linear sweep voltammetric (LSV) investigations are used to determine the PbO potential region in sodium sulphate solutions. An a.c. equivalent circuit is developed according to theoretical models for the metal/solid-electrolyte interface [6 - 9] and an exponential distribution of R–C elements [10, 11]. The potential dependence of the major circuit elements for pure Pb and Pb–6wt.%Sb alloys in the potential interval -0.8 to $+0.9$ V (the PbO-stability potential region *versus* Hg/Hg_2SO_4) is used to demonstrate the influence of antimony on both the interfacial processes and on the properties of the oxide film.

Experimental

The working electrodes consisted of smooth discs made from pure (99.99%) lead and Pb–6wt.%Sb alloy. The electrodes had a working surface area of nearly $1\ cm^2$ and were inserted in a Teflon support. The preliminary treatment consisted of mechanical polishing and electrochemical reduction at -1.2 V *versus* Hg/Hg_2SO_4 (for removal of oxidation products). Note, all potentials given in this paper are measured against an Hg/Hg_2SO_4 reference electrode. During voltammetric measurements, a platinum wire was used as a counter electrode, while for the impedance investigation a platinized-platinum electrode with a large real surface was employed. The forming electrolyte comprised $1\ M\ Na_2SO_4$, prepared from AR sodium sulphate and double-distilled water. The LSV curves were obtained over the potential region -1.3 to $+1.3$ V at a sweep rate of $1\ mV\ s^{-1}$ using a Radelkis OH-405 potentiostat connected to a Goertz SE 790 X–Y recorder. The impedance measurements were performed on a computer-controlled PAR M378 Impedance System over the frequency range 0.1 Hz - 100 kHz. The latter range was limited because of:

(i) poor reproducibility of the measurements in the lower frequency region due to the extended calculation time of the Fast Fourier transform;

(ii) the non-stationary condition of the system caused by PbO dissolution in the forming electrolyte.
The a.c. amplitude was < 5 mV and the d.c. potential interval was -0.8 to $+0.9$ V after a preliminary polarization at 0 V.

Results and discussion

LSV measurements

Cyclic voltammograms for pure lead and Pb–6wt.%Sb electrodes in 1 M Na$_2$SO$_4$ solution are given in Fig. 1. The anodic peak, A1, at -0.85 V represents the dissolution of lead to Pb^{2+} ions together with PbO formation and passivation. The maximum current density and the quantity of charge passed are both greater for pure lead than for the Pb–Sb alloy, i.e., a greater amount of PbO is formed on the pure lead. The anodic current peak, A2 (at ~ -0.5 V), on the Pb–6wt.%Sb voltammogram indicates the dissolution of antimony to Sb(III) soluble species; this is stopped by surface blockage due to PbO and Sb$_2$O$_3$ formation at potentials higher than -0.4 V. The passive state for pure lead is stable between -0.5 and $+0.75$ V. At more positive potentials, a further anodic peak, A3, appears due to Pb(II) oxidation and oxygen evolution (the latter predominates at higher potentials). The passive region is more extended (-0.2 to $+1.2$ V) for the alloy electrode and the steady-state current is greater.
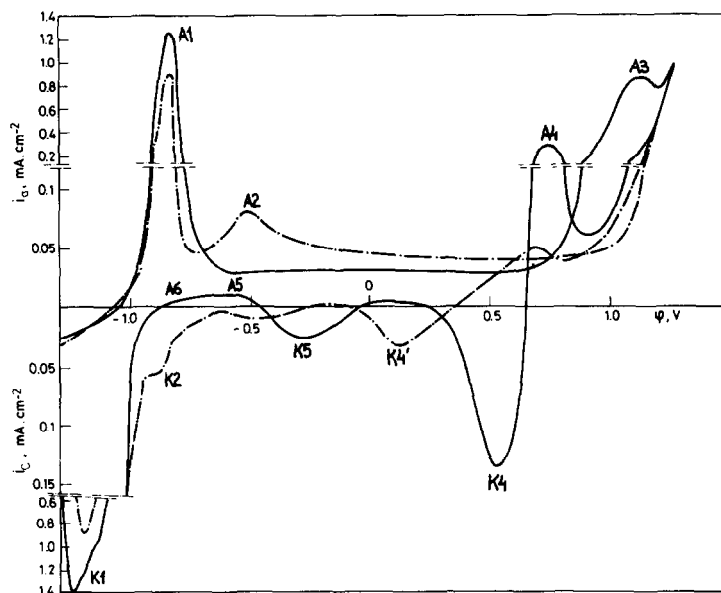

Fig. 1. Cyclic voltammograms for pure lead (——) and Pb–6wt.%Sb (– · – · –) in 1 M Na$_2$SO$_4$.

The negative-going (reverse) LSV scan for pure lead exhibits, in succession, an anodic peak, A4, and a cathodic peak, K4. It appears that further oxidation of Pb(II) to Pb(IV) is due to the diffusion of oxygen-containing species and water through the PbO layer and the formation of a surface, non-stoichiometric, oxide, part of which is reduced by chemisorbed OH^- ions at the film/solution interface. These processes are also observed for the alloy electrode, but the peak currents are much smaller and the potential of the K4' peak is much more negative than that for the K4 peak on pure lead. At lower potentials, a further reduction peak, K5, is observed on pure lead. This suggests that a partial reduction of Pb(IV) to Pb(II), and perhaps to pure lead, takes place. The latter may be supported by the secondary two-step oxidation (A5 - A6) that is observed at almost the same potential as that of the primary Pb/Pb(II) oxidation. For the alloy electrode, this secondary oxidation is masked by the cathodic peak, K2, for Sb(III) reduction. The main reduction peak, K1, for pure lead is almost twice the size of that for the lead–antimony electrode, *i.e.*, reduction of non-stoichiometric oxide takes place only on pure lead (no detectable amounts of Pb(IV) are formed on the alloy electrode).

From the above experimental results, it is concluded that two main parallel processes take place in the PbO potential region, namely, oxide-film growth under steady-state conditions, and solid-state diffusion of oxygen-containing species through the film that results in a lead-valency increase (the latter process is inhibited by the presence of antimony in the alloy).

a.c. Impedance measurements

The experimental impedance spectra Re(Z)–Im(Z) (*i.e.*, the imaginary part of the complex impedance as a function of its real part) for d.c. potentials of 0.2, 0.4 and 0.6 V are shown in Fig. 2(a) and (b) for pure lead and lead–antimony electrodes, respectively. The experimental results were processed by means of a programme package for a.c. equivalent circuits synthesis. Verification of the circuits and optimization of the parameter values were conducted using the Marquardt algorithm for non-linear least-squares analysis. The validity of two a.c. analogue circuits was established.

The first circuit was derived from the general a.c. circuit for a metal/solid-electrolyte interface, and the second circuit included a so-called CPA (constant phase angle) impedance (a two-parametrical element that signifies the existence of a particular type of energetic heterogeneity of the electrode surface). The two equivalent circuits are shown in Fig. 3(a) and (b). The corresponding (simulated according to the optimization procedure) impedance spectra are presented in Fig. 2(a) and (b) by the continuous solid lines. The close agreement between the experimental points and the simulated curves demonstrates the capability of these analogue circuits to reflect adequately the electrochemical properties of the investigated system.

To describe in a more detailed way the physical meaning of the main elements of the electrical circuit, a model for the mechanism of the overall oxidation reaction taking place on the lead substrate in sodium sulphate
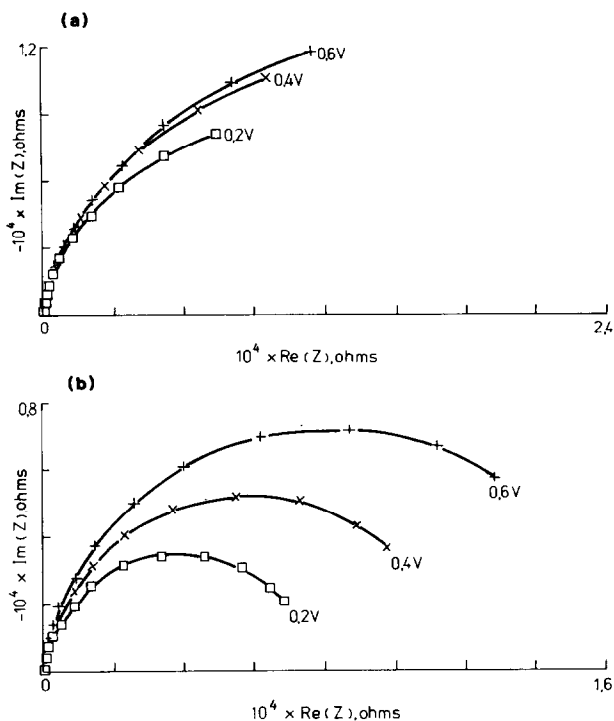
Fig. 2. Experimental (points) and calculated (solid lines) impedance spectra for: (a) pure lead; (b) Pb–6wt.%Sb.

solutions is proposed (in Fig. 4) (see also refs. 19, 20). Since the purpose of the present paper is to characterize the lead monoxide as a solid electrolyte, emphasis is placed on the processes at the Pb/PbO interface. Both oxygen vacancies and electrons are generated by the PbO formation. In the theory of a.c. equivalent circuits, electron transfer is represented by a charge-transfer resistance, R_t. The oxygen vacancies as main ionic current carriers are adsorbed at the interface [6]. Thus, an adsorption capacitance, C_a, is included in the electric circuit followed by a diffusion impedance, W_a, characterizing the diffusion of the major charge carriers (Fig. 3).

A multi-step half reaction of oxygen reduction proceeds at the PbO/solution interface. This process results in the formation of O^{2-} ions. The latter diffuse through the bulk of the film at a rate that can be evaluated from the values of the second Warburg impedance constant, W. The surface at which an oxygen anion and a vacancy meet is the reaction surface with the maximum concentration of charge carriers.

The stability of the passive state in the PbO potential region can be determined from the potential dependence of the main components of the a.c. circuit. Information about the nature of the processes in the steady-state potential range can also be collected. In this connection, two methods for
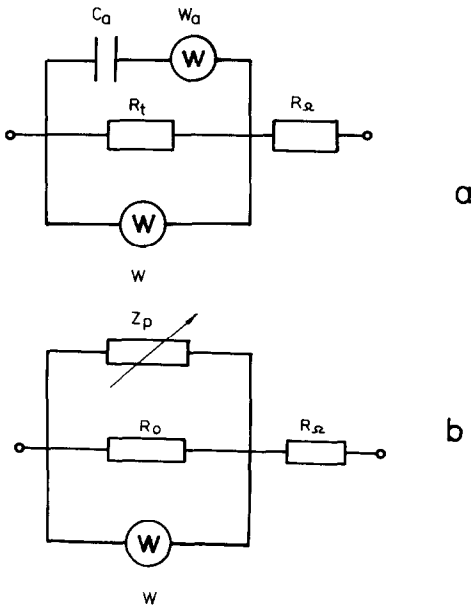
Fig. 3. Proposed equivalent circuits: (a) metal/solid electrolyte interface; (b) including CPA impedance.

obtaining this dependence are adopted after first conducting a preliminary polarization at 0 V until a steady state is reached. In the one method, steps to more positive potentials are applied, while in the other method, steps to more cathodic potentials are applied. For the positive-going ('oxidation') steps, the potential dependence is illustrated in Figs. 5 and 6 for the circuit components of Fig. 3(a) and in Fig. 7 for some circuit components of Fig. 3(b). The same dependences, but for the negative-going ('reduction') steps are shown in Figs. 9 - 11.
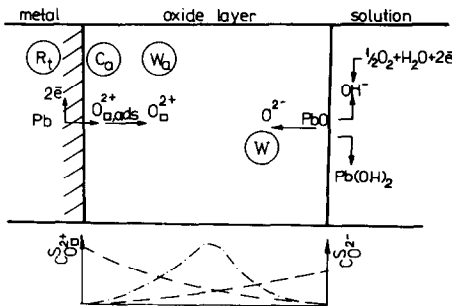

Fig. 4. Proposed model for overall oxidation reaction of lead in Na_2SO_4: physical meaning of the equivalent-circuit parameters.
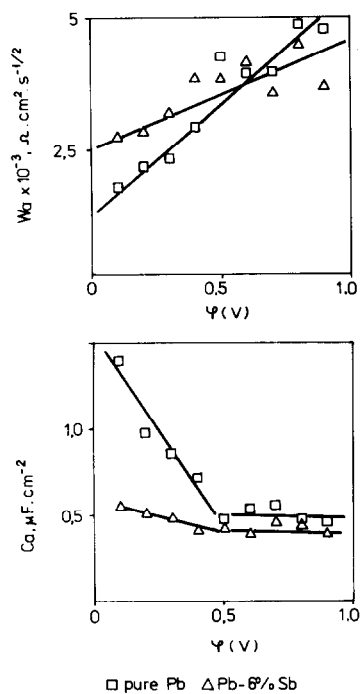
Fig. 5. Potential dependence of Warburg constant (W_a) and capacity (C_a) of adsorption in PbO-stability potential range. Application of oxidation steps.

An examination of the potential dependence when using positive-going potential steps provides basic information on the oxidation process mechanism and the ratio between different rate-determining steps. For both pure lead and Pb–Sb alloy, the capacity of the major carriers reaches a constant value for potentials higher than 0.5 V, *i.e.*, the degree of coverage of the electrode surface with oxygen vacancies remains constant. The diffusion impedance of the charge carriers, W_a, increases with the polarization. Thus, the passive state is stabilized (*i.e.*, the diffusion rate slows down), see Fig. 5.

For a pure lead electrode, the charge-transfer resistance, R_t, which characterizes the faradaic process in the passive state, shows a maximum at a potential close to 0.6 V (Fig. 6), and then rapidly decreases. According to the LSV for pure lead (Fig. 1), a new process of oxidation begins at higher potentials. For the Pb–6wt.%Sb electrode, at potentials above 0.6 V, the resistance R_t increases more sharply, *i.e.*, a new process cannot be distinguished. The suggestion that R_t and W describe different stages of one and the same process can be confirmed by studying the potential dependence of W. The values of this diffusion constant for pure lead and lead–antimony both exhibit a maximum close to 0.5 V, with the same rapid decrease thereafter, but are almost twice as large for the alloy electrode. It is concluded, therefore, that the presence of antimony inhibits the diffusion step of the
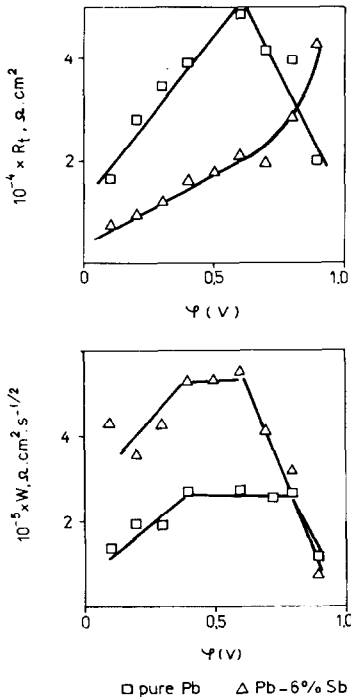
Fig. 6. Potential dependence of charge-transfer resistance (R_t) and second Warburg constant (W) in PbO-stability potential range. Application of oxidation steps.

reaction and that this inhibition, in turn, is due to the lower ionic permeability of the formed layer (a prior formation of a non-conductive passive film of antimony (III) oxide could also be imagined).

The applicability of a circuit closely related to the one shown in Fig. 3(b) for the system $Pb/PbO/PbSO_4/H_2SO_4$ is discussed in ref. 18. In this work, a study is made of the dependence of the illumination intensity of the overall impedance, as well as of the resistance of the film bulk, on the CPA impedance constant. For a pure lead electrode, the equivalent circuit shown in Fig. 3(b) differs from that described in ref. 18 only by the presence of the Warburg constant W (it could not be identified for the lead–antimony electrode). The circuit includes the so-called CPA impedance, which is defined by the equation:

$$Z_p = K_p(jw)^{-p} \tag{1}$$

where K_p is a constant defined in the same way as the Warburg constant, but with a phase shift of $p(\pi/2)$ degrees. This kind of two-parameter element, as well as the Young capacity [17] and the infinite exponential distribution of R–C elements [10], describes a particular type of energetic heterogeneity of the electrode surface, or at the electrode/electrolyte interface (adsorption of surface-active species, diffusion-controlled faradaic reaction proceeding at
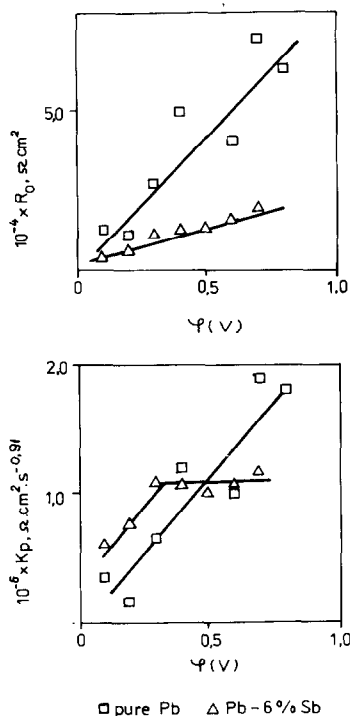
Fig. 7. Potential dependence of bulk film resistance (R_0) and CPA impedance constant (K_p) in PbO-stability potential range. Application of oxidation steps.

so-called active sites on the electrode surface, distribution of surface states at the semiconductor/electrolyte interface, etc.). The potential dependence of the CPA impedance constant, K_p, and of the film bulk resistance, R_0, is given in Fig. 7. It can be seen that for a pure lead electrode, there is a nearly linear increase in the parameters. This confirms that the charge-transfer reaction and the diffusion slow down as the anodic polarization increases. In the case of the lead–antimony electrode, only the resistance of the oxide film, R_0, increases linearly. By contrast, K_p reaches a constant value at potentials above 0.4 V (the parameter p is almost independent of the potential and has a value of ~ 0.91). Assuming that the CPA is associated with the adsorption–diffusion of vacancies at the Pb/PbO interface, it can be concluded that a steady state is reached for the alloy electrode. The potential dependence of R_0 leads to the conclusion that the film growth on the alloy electrode is slower and the thickness of the layer is smaller. This fact could also be explained by a prior formation of a non-conductive passive Sb_2O_3 layer. The most important fact is, however, that the second Warburg constant cannot be identified in the case of the alloy electrode. This illustrates the inhibiting effect of antimony on the diffusion step in the overall PbO-formation process.
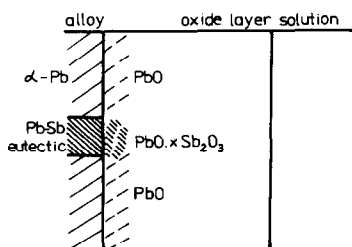
Fig. 8. Heterogeneity of oxide layer: lead monoxide and antimony–lead oxide zones.

A model for the heterogeneity of the alloy substrate surface can be employed in order to clarify the influence of antimony on the oxide formation. A schematic of such a simplified model is given in Fig. 8. It is well known that the alloy material is a eutectic mixture of α-lead and lead–antimony. The lead monoxide is formed on both substrate regions, but on the eutectic it is possible that the formation of Sb_2O_3, as well as of a mixed antimony–lead oxide (shown in Fig. 8 as $PbO \cdot xSb_2O_3$) can occur.

Further evidence for the formation and reduction of antimony(III) oxide can be obtained by studying the potential dependence of the major circuit
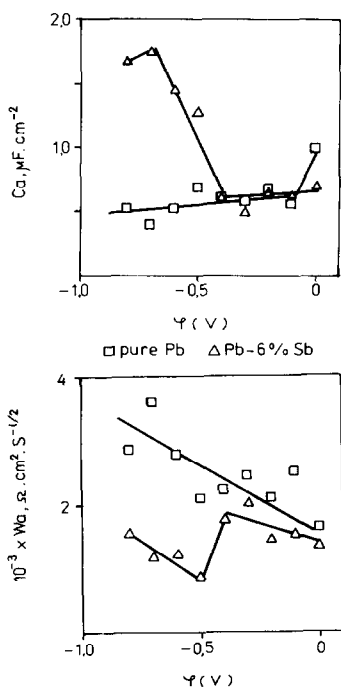

Fig. 9. Potential dependence of capacity (C_a) and Warburg constant (W_a) of adsorption in PbO-stability potential range. Application of reduction steps.
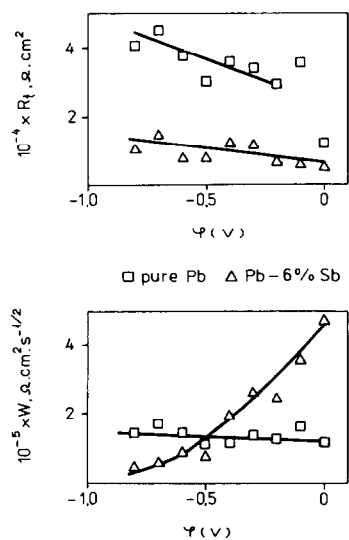
Fig. 10. Potential dependence of charge-transfer resistance (R_t) and second Warburg constant (W) in PbO-stability potential range. Application of reduction steps.
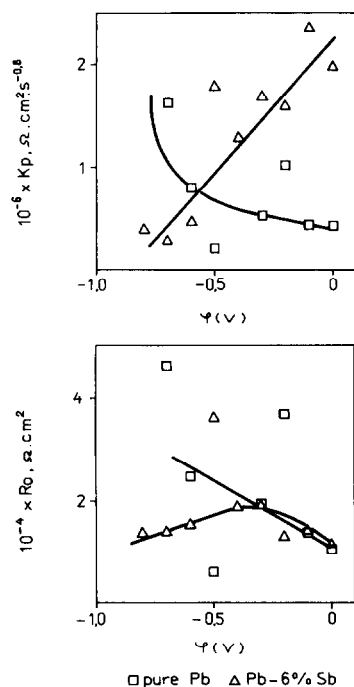

Fig. 11. Potential dependence of CPA impedance constant (K_p) and bulk-film resistance (R_0) in PbO-stability potential range. Application of reduction steps.

elements resulting from the data of negative-going steps. These dependencies are illustrated in Fig. 9 for the adsorption parameters of the major carriers (C_a and W_a), in Fig. 10 for the faradaic process parameters (R_t and W), and in Fig. 11 for the elements of the second electrical circuit of Fig. 3(b) (K_p and R_0). For the pure lead electrode, most parameters show a slightly pronounced potential dependence. This demonstrates the stability of the passive state over a wide potential range. For the lead–antimony oxide electrode, the potential dependence of the adsorption parameters (Fig. 9) exhibits a sharp change near -0.5 V. This fact can be connected with a change in the concentration of oxygen vacancies that results from the antimony(III) reduction taking place at potentials close to -0.5 V. The decrease of the adsorption Warburg constant W_a is obviously a consequence of this reduction process. The change in vacancy concentration due to the Sb(III) reaction results in an increase in the diffusion rate of O^{2-} ions. The latter which is observed clearly in Fig. 10 shows the potential dependence of W. For the pure lead electrode, the value of W is almost constant over the entire range (-0.8 to 0 V) while for the alloy, a sharp decrease in W values is observed. These results are confirmed also by the shape of the potential dependence of K_p and R_0 (Fig. 11); this demonstrates a significant difference between the oxide-layer stability on the two types of electrode. For the resistance of the bulk film, a slow increase down to -0.5 V is transformed into a decrease at more negative potentials, apparently because of the higher conductivity of the lead–antimony oxide layer (due to the reduction of Sb(III)).

Taking account of all the above results, it can be concluded that the formation of an antimony–lead oxide layer on the alloy substrate is the main cause of the passive state stability. The layer strongly influences the solid electrolyte and mass-transfer properties of the electrode system under investigation. The oxide film can also determine the mechanism of further Pb(II) oxidation and thus play an important role in the corrosion layer processes during the operation of lead/acid batteries.

Conclusions

The electrochemical behaviour of both the $Pb/PbO/Na_2SO_4$ and the $Pb–Sb/(Pb–Sb)O/Na_2SO_4$ electrode systems has been investigated using the LSV and a.c. impedance techniques. Two types of a.c. analogue circuit have been proposed and by using computer simulation and optimization of the parameter values, the applicability of these circuits has been verified. The potential dependence of the major circuit components has been established in the potential range of PbO stability by LSV measurements. On the basis of this dependence, it can be concluded that the passive film formed on Pb–Sb alloys has a higher stability, as well as less ionic conductivity, than the film on pure lead. The inhibition of the solid-state, diffusion-controlled reaction by the presence of antimony is also of great importance. The main conclusion, however, appears to be the definition of oxide layer heterogeneity in terms of

a possible formation of mixed antimony–lead oxide zones on the alloy substrate. This heterogeneity results in a change in the mechanism of oxidation/reduction under steady-state conditions — a fact that could be significant in studies of the influence of antimony on the performance of lead/acid batteries.

References

1 F. Mansfeld, M. W. Kendig and S. Tsai, *Corrosion*, *38* (1982) 570.
2 F. Mansfeld, *Corrosion*, *36* (1981) 301.
3 I. Epelboin, M. Keddam and H. Takenouti, *J. Appl. Electrochem.*, *2* (1972) 71.
4 S. G. Canagaratna and S. R. Karunathilaka, *J. Electroanal. Chem.*, *48* (1973) 183.
5 J. R. McDonald, J. Schoonman and A. P. Lehnen, *J. Electroanal. Chem.*, *131* (1982) 77.
6 E. A. Ukshe and N. Bukun, *Twerdie Elektrolity*, Nauka, Moscow, 1977.
7 S. H. Glarum and J. H. Marshall, *J. Electroanal. Chem.*, *132* (1982) 59.
8 U. V. Shirokov, P. D. Lukovcev and V. S. Borovkov, *Elektrochimiya*, *7* (1971) 3.
9 U. M. Povarov, L. A. Beketaeva and B. K. Puresheva, *Elektrochimiya*, *18* (1982) 10.
10 P. H. Bottelberghs and G. H. J. Broers, *J. Electroanal. Chem.*, *67* (1976) 55.
11 J. F. McCann and S. P. S. Badwal, *J. Electrochem. Soc.*, *129* (1982) 3.
12 N. A. Hampson, S. Kelly and K. Peters, *J. Appl. Electrochem.*, *11* (1981) 751.
13 S. Kelly, N. A. Hampson and K. Peters, *J. Appl. Electrochem.*, *11* (1981) 764.
14 M. Maja and N. Penazzi, *Electrochim. Acta*, *30* (1985) 6.
15 G. A. Kokarev, N. G. Bahchisaraitsyan, A. N. Smirnova and G. I. Medvedev, *Tr. MHTI im. Mendeleeva*, *54* (1967) 169.
16 H. Goehr, J. Soellner and H. Wienzierl, *34th I.S.E. Meeting, Erlangen, 1983*, 0715.
17 H. Weinzierl, Impedanzspektrometrische Untersuchungen der anodischen Bildung und kathodischen Reduktion von Bleisulfatschichten auf glatten Bleielektroden in Schwefelsaure, *Dissertation*, Erlangen-Nurnberg, 1988, p. 21.
18 Z. A. Rotenberg and N. V. Nekrasowa, *Electrochimiya*, *18* (1988) 11.
19 K. Laws, *J. Chem. Phys.*, *39* (1963) 8.
20 D. Pavlov, *Electrochim. Acta*, *23* (1978) 845.
21 D. Pavlov, *J. Electroanal. Chem.*, *118* (1981) 167.